Characterization of the multicellular membrane-bearing algae from the early Cambrian Kuanchuanpu biota

Yajuan Zheng[1]*, Qingqin Tang[2]*, Ping Liu[2], Jie Sun[2], Xiaoyong Yao[1], Wenjing Hao[2], Xiaoguang Yang[2], Junfeng Guo[1,2], Kentaro Uesugi[3], Tsuyoshi Komiya[4], Jian Han[2]

[1]School of Earth Science and Land Resources, Key Laboratory of Western China's Mineral Resources and Geological Engineering, Ministry of Education, Chang'an University, Xi'an 710054, China

[2]Shaanxi Key Laboratory of Early Life and Environments (SKLELE), State Key Laboratory of Continental Dynamics (SKLCD), Department of Geology, Northwest University, Xi'an 710069, China

[3]Japan Synchrotron Radiation Research Institute (JASRI), 1-1-1 Kouto, Sayo-cho, Sayo-gun, Hyogo, Japan

[4]Department of Earth Science and Astronomy, Graduate School of Arts and Sciences, The University of Tokyo, Tokyo 153-8902, Japan

Corresponding author: Jian Han (elihanj@nwu.edu.cn)

* These authors contributed equally

Key Points:

- Early Cambrian spherical embryo-like fossils are multicellular algae
- Multicellular algae exhibit a cortex-medulla-like differentiation
- An evolutionary continuity of algae during the Ediacaran-Cambrian Period.

Abstract

The diversity of small shelly fossils (SSF) demonstrates that multicellular organisms underwent large-scale radiation at the beginning of the Cambrian, which is highlighted by the coexistence of various metazoans and the occurrence of their embryo fossils. However, little is known about early Cambrian eukaryotic multicellular algae, the primary producers that replaced oxygenic cyanobacteria and played a crucial ecological role in matter cycling and energy dynamics in marine ecosystems. In this study, hundreds of microscopic three-dimensionally preserved multicellular agglomerate fossils were obtained from the early Cambrian Kuanchuanpu Formation (535 Ma) in southern Shaanxi, South China, which consisted of several tightly-packed multicellular clusters encapsulated within a thin organic membrane. Synchrotron tomography analysis further revealed that the cells of the whole agglomerate, although partitioned into different subunits by a gelatinous membrane, were distinctly differentiated into an outer conical cell layer and an inner spherical-cell layer, thus suggesting of a cortex-medulla-like differentiation. These characteristics resemble those of multicellular algae (e.g. *Wengania*, *Gremiphyca*, and *Thallophyca*) from the Ediacaran Weng'an biota (South China) in morphology, size, and internal cell structure. Furthermore, a potential asexual life cycle for these membranous algae was proposed based on their morphological and structural characteristics. Our findings support an evolutionary continuity of the multicellular algae from the Ediacaran to the early Cambrian Period.

1. Introduction

The chlorophyll-based photosynthesis of eukaryotic multicellular algae transformed the Proterozoic ocean-atmosphere system into its modern state (Butterfield, 2015; Tang et al., 2020). Particularly, the rise of algae, approximately 1,900 to 900 million years (Myr) ago (Sanchez-Baracaldo et al. 2017), in comparison with cyanobacteria made food webs more efficient in nutrient and energy transfer, driving the occurrence of larger and increasingly complex organisms (Brock et al., 2017). Recent studies on molecular biomarkers have indicated a rapid increase of multicellular algae (e.g. red algae and green algae) after the Cryogenian (Brocks et al., 2017). Moreover, abundant multicellular algae fossils dating from the Mesoproterozoic to the Ediacaran period were identified in the Indian plate (Kumar, 2001; Sharma et al., 2009; Sharma and Shukla, 2009, Bengtson et al., 2017), North America (Walter et al., 1976, 1990), and the Yangtze plate (Zhu et al., 2016; Ding et al., 1992; Tang et al.,1997; Wang et al., 2007; Zhang, 1989; Xiao et al., 2002; Yuan et al., 2001, 2016; Zhao et al., 2004; Tang et al., 2007). However, most algae fossils are usually preserved as macroscopic compressed carbonaceous films without cellular structures, except for the fossils obtained from the Lower Vindhyan in central India (Bengtson et al., 2017) and the Ediacaran Doushantuo Formation in South China (Zhang, 1989; Zhang and Yuan, 1992). In particular, the Doushantuo phosphorites contain an exceptional record of multicellular algae featuring many anatomical and reproductive features seen in the modern marine flora such as conceptacle, spermatangia, and a cortex-medulla differentiation (Zhang, 1989; Zhang and Yuan,1992; Zhang et al. , 1998; Xiao et al., 1999). These fossils provide an exceptional opportunity

to understand the evolution and diversification of algae in Neoproterozoic marine ecosystems during the advent of the Ediacaran metazoan radiation.

Cambrian fossil algae are quite abundant. They are preserved as macroscopic compressed carbonaceous films in Burgess shale-type Lagerstätten in south China, including the Chengjiang (Hou et al., 2017), Balang (Yang et al., 1999, 2001), Yanjiahe (Guo et al., 2011), and Qingjiang biotas (Fu et al., 2019). Additionally, they were also found in cherts (Yin, 1987; Shang et al., 2020) or phosphatized rocks (Shen, 1987) alongside various small shelly fossils. Although algae have been an essential component of the Cambrian marine ecosystem, they were largely neglected, and their role during Cambrian metazoan radiation was poorly investigated.

The early Cambrian Kuanchuanpu biota in Southern Shaanxi Province China (Fig. 1a–c) constitutes a complete ecosystem, which not only contains small shell fossils (Qian, 1999; Li, 1992) and animal embryos (Yue and Bengtson, 1998; Bengtson and Yue, 1997; Zhang et al., 2015; Han et al., 2017)(Fig. 1d), but also up to ten species of microbial cyanobacteria (Ding, 1986; Yin, 1987; Qian, 2007; Liu et al., 2014; Yang et al., 2017; Cui et al., 2020), and spherical coccoidal bacteria colonies (Steiner et al., 2004a). However, the algae were seldom documented, and hardly be distinguished from animal embryos in the cleavage stage. Zheng et al. (2017) reported multicellular spherical fossils with tetrad division and cellular structure, which were highly comparable to eukaryotic algae fossils from the Weng'an biota. Nevertheless, this study only characterized basic morphological features and did not demonstrate the internal structures for further biological classification.

Here we presented the morphology and internal microstructure of multicellular membrane-bearing algae from the early Cambrian Kuanchuanpu biota using a scanning electron microscope (SEM) and synchrotron radiation X-ray tomographic microscopy (SRXTM). Our findings reveal a cell differentiation of algae thalli, and provide a theoretical basis for the systematic classification of these multicellular algae in comparison with those of the Weng'an biota.

2. Stratigraphy

All samples were collected from the Shizhonggou section of the Lower Cambrian Kuanchuanpu Formation in Ningqiang County, southern Shaanxi, China (Fig. 1a–c). This region comprises a series of shallow sea carbonate deposits of the Yangtze Platform, which is in turn primarily composed of dark grey or black phosphorus limestones interbedded with thin layered chert. In this section, the bottom of the Kuanchuanpu Formation is disconformably underlain by the gray-white dolomite at the top of the Ediacaran Dengying Formation (Bengtson and Yue, 1992). There is also a disconformity between the Kuanchuanpu Formation and the overlying siliciclastic Lower Cambrian Guojiaba Formation characterized by gray-dark silty shale. The Kuanchuanpu Formation is approximately 60–70 meters thick and rich in small shelly fossils and animal embryos (Fig. 1d), and is chronologically equivalent to the first small shelly fossil as-

semblage zone (i.e., the *Anabarites trisulcatus–Protohertzina anabarica* Zone) of the Fortunian Stage and Terreneuvian Series (see Fig. 2 in Steiner et al., 2004a).

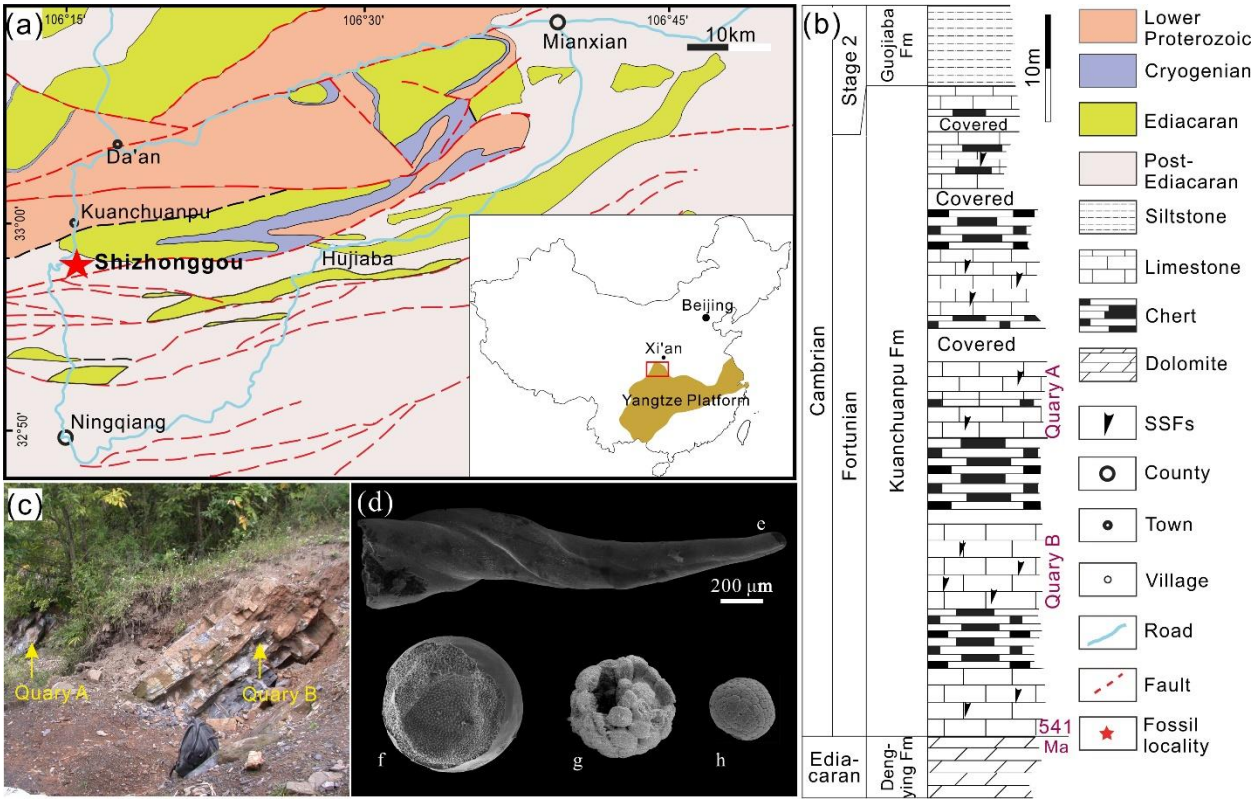

Figure 1. Geological map, stratigraphy, and typical fossils from the Shizhonggou section in Ningqiang County, Shaanxi Province. (a), a geological map showing the Cambrian strata and the fossil locality (modified from Han et al., 2016a). (b), stratigraphic column of the Shizhonggou section in Ningqiang. (c), A photograph showing two quarries of the rock samples. (d), Micro-fossils from the Shizhonggou section: e, *Anabarites*, specimen No. ELISN001-K31-102; f, an embryo of *Olivooides*, No. ELISN138-5; g, an animal embryo in the gastrulation stage (From Yasui et al., 2013); h, an embryo-like fossil, No. ELISN012-K31-098. Fm: formation.

3. Materials and methods

The rock samples were treated with 5%–10% acetic acid and manually selected under a binocular stereoscopic microscope. The 117 selected specimens, coated with gold, were then observed and measured using a SEM of FEI Quanta 400 FEG with a 20 kV voltage. Two samples (ELISN004-51, ELISN159-297) were analyzed using SRXTM at SPring-8 (Hyogo, Japan). The specimens were imaged through 360◦ rotation. 3D reconstructions of X-ray data and movies, were conducted using the Dragonfly 4.1software. All specimens are deposited at the SKLELE of Northwest University, Xi'an, China.

4. Results

4.1. External morphology of the multicellular agglomerate fossils

The multicellular membrane-bearing agglomerate fossils are found to be amorphous in shape (Figs. 2, 3; Movie S1, S2), variable in size, and are constituted by several multicellular sphere-shaped or clump-shaped multicellular units that formed a secondary population (Figs. 2,3; Movie S1, S2). The length of the 117 specimens studied herein ranges from 500 μm to 2900 μm (blue bar in Fig. 4) and are 1230 μm on average, but most specimens range from 800 to 1400 μm. Their widths range from 350 to 2000 μm (red bar in Fig. 4) with a 500–1000 μm dominance and an average of 820 μm (Fig. 4). Some of the multicellular units in the agglomerates are regular spheroid (Fig. 3c), papillary (arrows in Fig. 3a, h), or rather irregular in shape (Figs. 3a, h and 5a). These multicellular units range from 30 to 500 μm in diameter (350 μm on average).

Light microscopy imaging shows that the microfossil agglomerate is encapsulated by a thin and smooth primrose yellow or white membrane layer, closely attached to the multicellular units (Fig. 2a). The organic membrane, approximately 1 μm in thickness, is mostly visible in the recessed area (Fig. 2d–h). The membrane is inconspicuous between two multicellular clumps (Fig. 6d, white arrow), but became much thicker at the triangular intersection between three or four multicellular clumps (Fig. 6i).

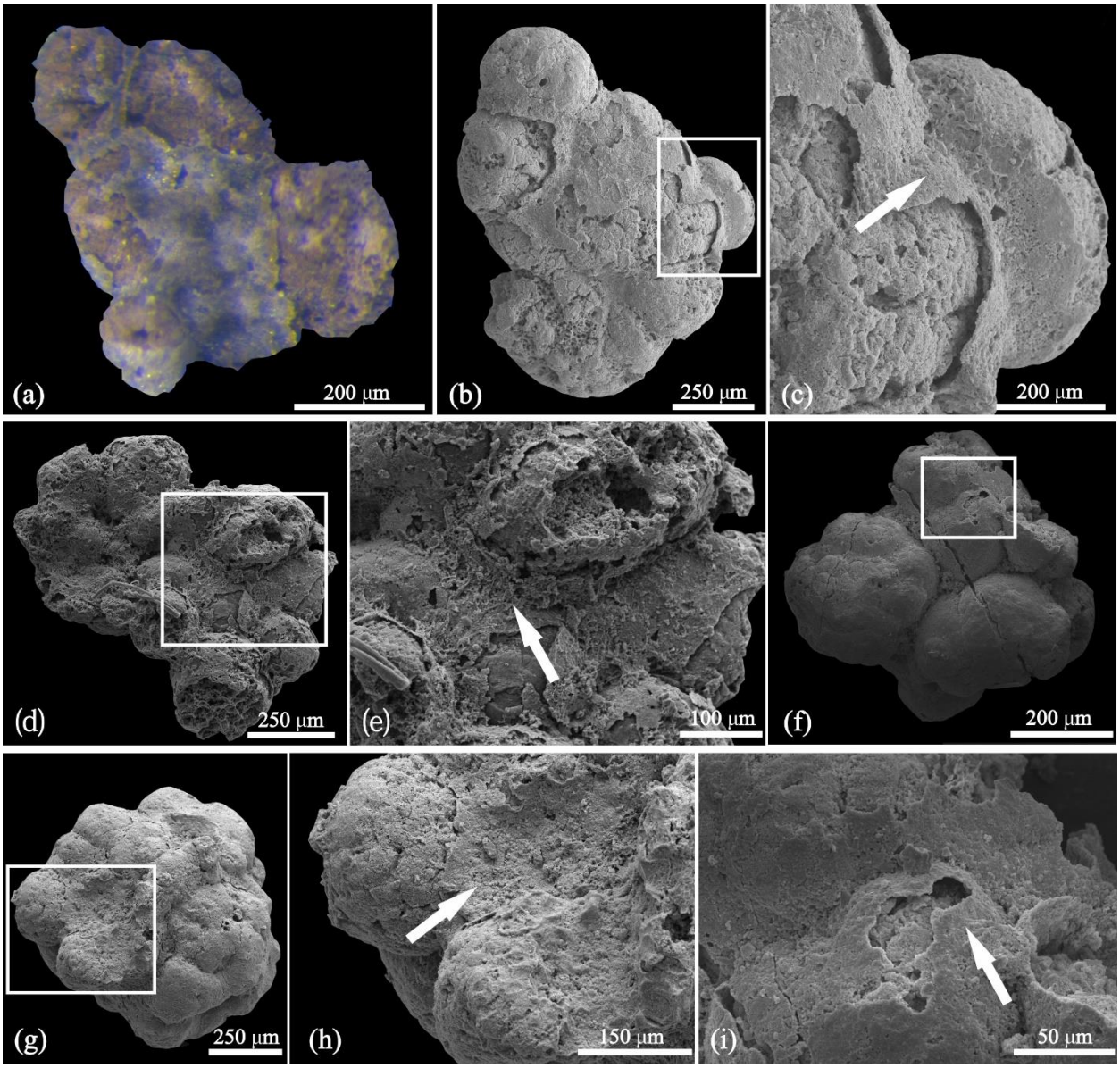

Figure 2. External membrane of multicellular agglomerate fossils from the Cambrian Kuanchuanpu Formation. (a), optical microscope imaging shows a smooth pale-yellowish external membrane. (b–i), SEM imaging shows the decay of the external membrane. (c, e, h, and i), close-up views of the areas marked by frames in (b, d, g, and f), respectively. (a–c): specimen No. ELISN160; (d and e): specimen Nos. ELISN160 and ELI SN140-224; (f and i): specimen No. ELISN160-203; (g and h): specimen No. ELISN159-297.

The multicellular units in the agglomerate fossils are tightly or loosely connected. Some irregularly shaped units, bordered by evident cleavage depressions, are closely interconnected to each other (Fig. 3c, f); whereas some larger units are loosely connected to the agglomerate and

even partitioned by the organic membrane, making them an independent unit within the agglomerate (Fig. 3g).

On the surface of some large multicellular units, the cleavage furrows are discernible in a hierarchy based on length and depth (Fig. 3b). The deeper and broader furrows (df) divided the unit into subunits, and the shallower, shorter ones (sf) in the subunit continued to divide the cell groups into clear-cut polygonal single cells approximately 30 μm in width (Fig. 3e), which is reminiscent of cell division sequences. Some inconspicuous cleavage furrows could be recognized due to the presence of prominent hemispherical or clump-shaped subunits on the agglomerate surface (Fig. 3b, c).

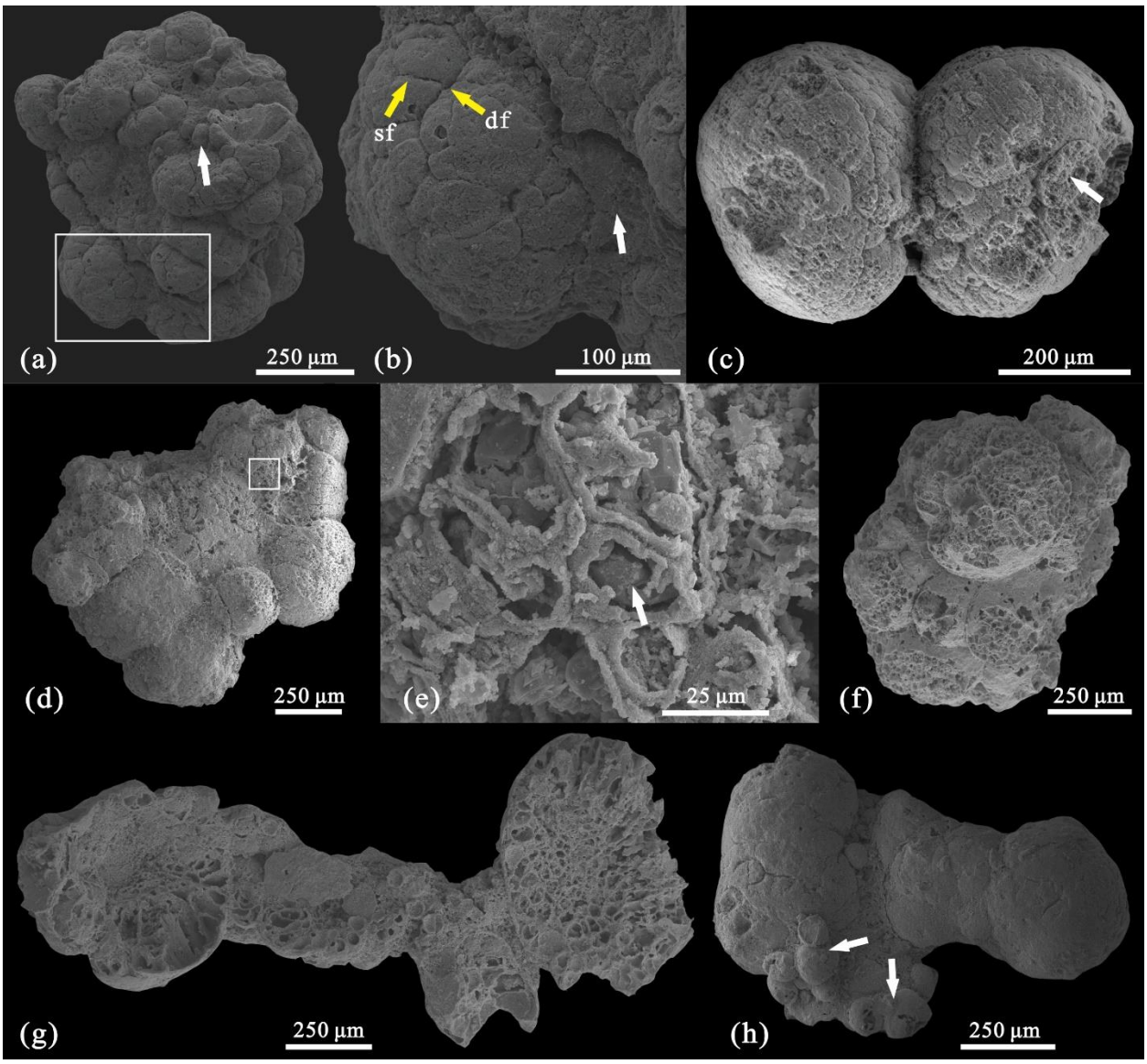

Figure 3. External morphology of multicellular agglomerate fossils from the Cambrian Kuanchuanpu Formation. (a–h), Multicellular agglomerate fossils (ELISN160-413,

ELISN160-k31, ELISN164-294, ELISN167-244, ELISN160-153, ELISN160-310). (a) Multicellular clump and mammillary clump (white arrow) size variations. (b) close-up view of the area marked by the frame in A, which shows the fragmentary membrane between the units (white arrow) and different depth cleavage wrinkles (yellow arrows). (c), double spherical-like agglomerate fossils and smaller multicellular units (white arrow) in the sphere. (d and e), multicellular agglomerate. (e), close-up view of (d) and polygonal cell (white arrow). (f), multicellular agglomerate without a preserved membrane, the latticed holes indicate single cells with broken walls. (g), loosely connected agglomerate and the organic membrane (white arrow) that divides the multicellular units. (h), agglomerate with nipple-like multicellular units (white arrows). df: deep furrow; sf: shallow furrow.

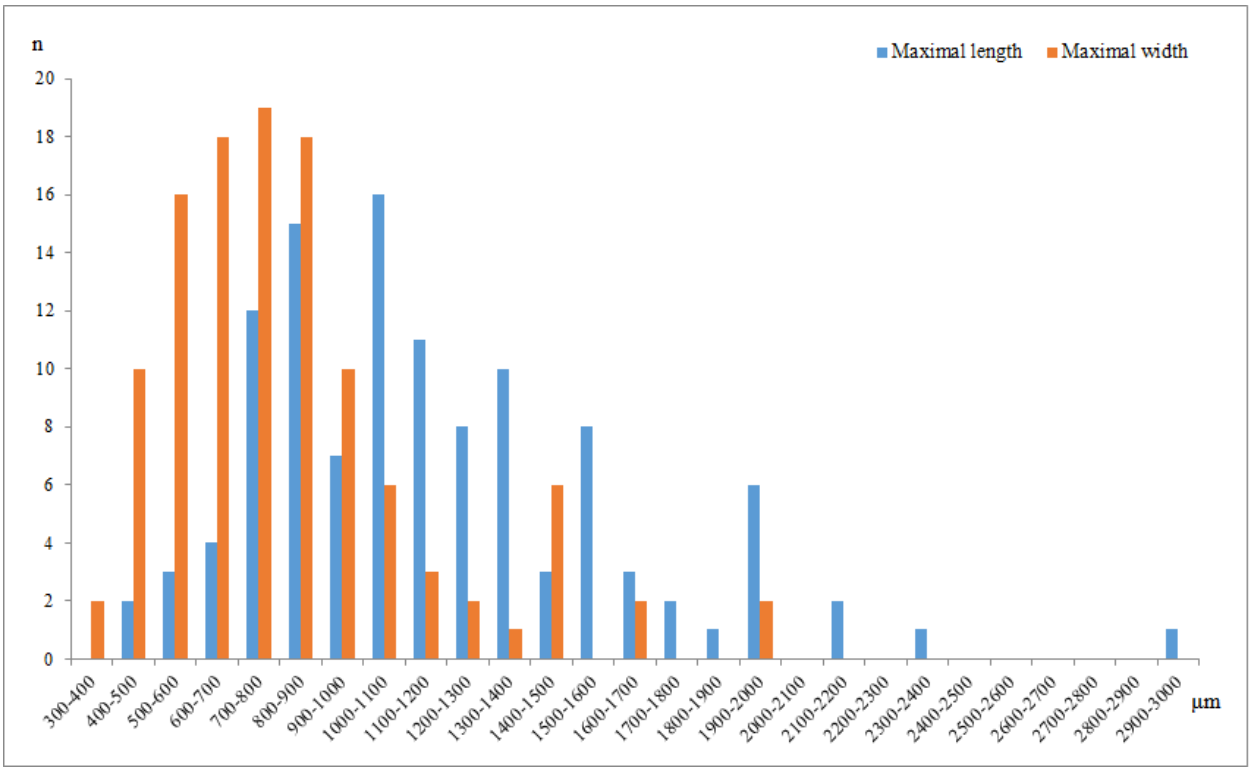

Figure 4. Size distribution of agglomerate fossils from the early Cambrian Kuanchuanpu Formation in South China. Agglomerate fossil length (blue bars); agglomerate fossil width (red bars).

4.2. Internal morphology of multicellular agglomerate fossils

The SRXTM results are mostly consistent with the light microscopy or SEM observations that the amorphous agglomerate is constituted by several different-sized multicellular clump-shaped units with distinct boundaries (Fig. 5; Movie S1, S2). Moreover, the clump-shaped units in the virtual cross section are further divisible as superficially triangular or trapezoid sections (Fig. 5b–e, g–i). On loosely connected multicellular units, the outer membrane may more or

less extend into the lumps, and the converging of the thin membrane in adjacent multicellular units may fuse into a substantially thicker non-cellular gelatinous membrane (gm) (Fig. 5b, c, g).

Interiorly, however, the cell clusters of the whole agglomerate, although partitioned into different subunits by the gelatinous membrane, are distinctly differentiated into an outer and an inner layer (Movie S1, S2). The outer cells are closely aligned at the peripheral region of the agglomerate with clear axial intercellular boundaries directed towards the agglomerate center (Fig. 5i). These structures are equivalent to the above-mentioned triangular or trapezoid sections in the virtual cross section, which are approximately 15 μm in width and 50 μm in axial length, with a length-width ratio ranging from 1:3 to 1:4. The outer cells contribute approximately half of the agglomerate volume. The triangular or trapezoid sections are further subdivided into multiple cells. In contrast, the cells in the inner layer of the whole agglomerate or multicellular clump are indivisible into secondary groups. These cells are spherical or spherical-like/spindle-like, exhibited uniform shape, and are approximately 5 μm in diameter, significantly smaller and uniform in size in comparison with the outer layer cells (Fig. 5e, j).Notably, the cell boundaries in some areas are obscured by the development of numerous hollow wormhole-shaped ambient inclusion trails (AITs) (Fig. 5b–e) that were produced in the early diagenesis (see Yang et al., 2017).

4.3. Organic outer cell wall of the agglomerate fossils

The cellular structure in the multicellular clumps with broken surfaces is well exposed using SEM (Fig. 6). The outer layer within the clump interior is composed of a tightly-packed ring of cylindrical or square-column cells (indicated by two concentric circles in Fig. 6b) with lateral cell walls directed toward the clump center; whereas the surface view of the clump exhibits a honeycomb pattern like traditional Chinese "window lattice" (Fig. 6e–j) as the lacking of cytoplasm and organelles. Each honeycomb structure represents a single cell, approximately 50 μm in width. A shared cell wall, approximately 1.5 μm in thickness, is visible between two adjacent cells. Whereas in some specimens, a narrow gap is observed between adjoining cell walls (white arrow in Fig. 6c–d). In contrast, the inner cell walls, as viewed via SEM and SRXTM, are much smaller; they are spherical in shape and are arranged in a reticular pattern (Fig. 6b, i; Movie S1, S2).

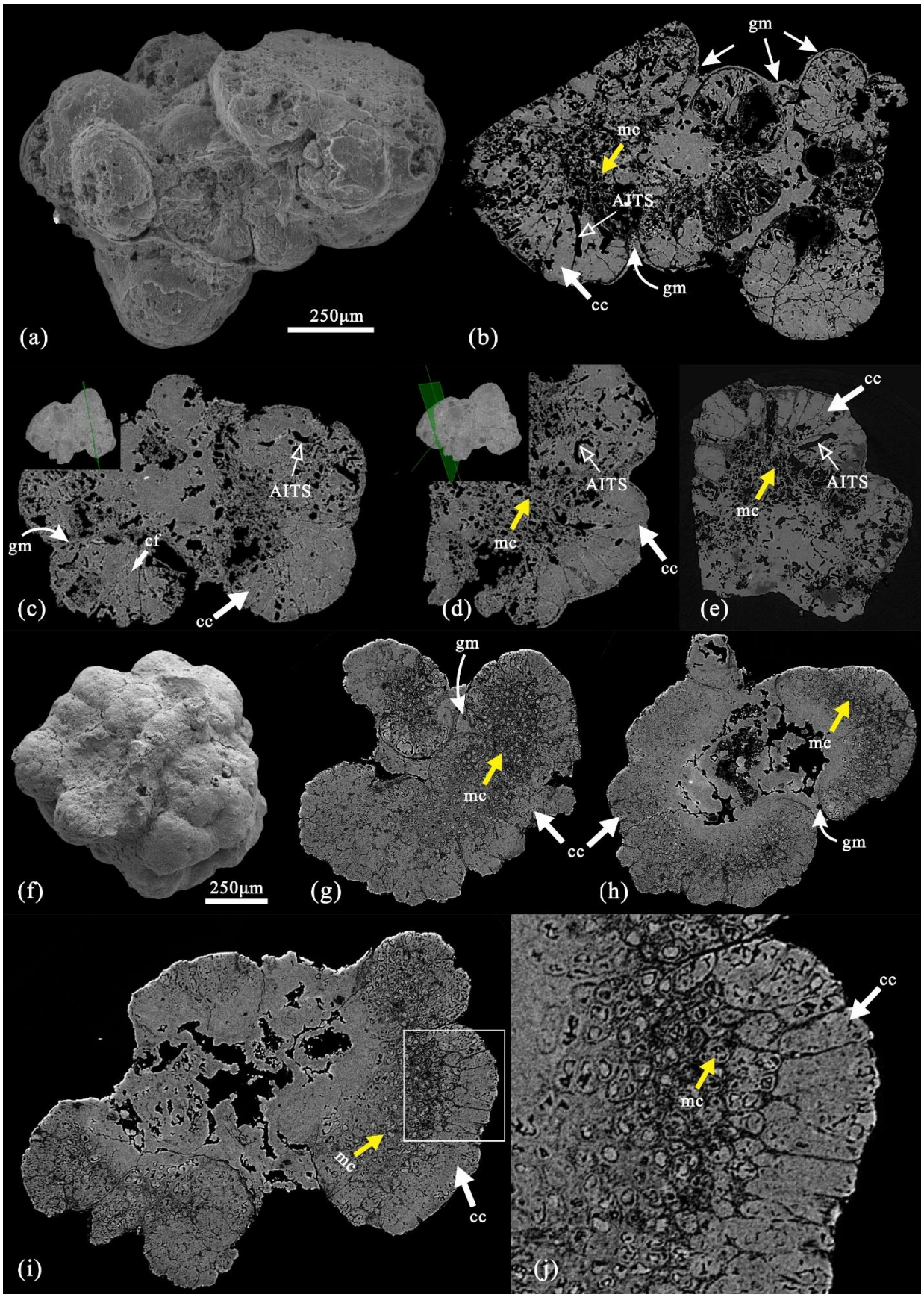
gm
mc
AITS
gm
cc
250µm
(a)
(b)
AITS
gm
cf
cc
(c)
AITS
mc
cc
(d)
cc
AITS
mc
(e)
(f)
250µm
gm
mc
cc
(g)
mc
gm
(h)
mc
cc
(i)
cc
mc
(j)

Figure 5. Interior anatomy of multicellular agglomerate fossils from the Cambrian Kuanchuanpu Formation. (a–e), No. ELISN004-k30-51, multicellular agglomerate fossils. (a) SEM image; (b–e), virtual sections of SRXTM of (a). (f–j), No. ELISN159-297, multicellular agglomerate fossils; (f) SEM image; (g–i), virtual sections of SRXTM of (f); (j), close-up views of areas marked by frames in (b3), which show cellular units. AITs: ambient inclusion trails; cc: cortical cells; cf: "cell fountain"; gm: gelatinous membranes; mc: medullary cells.

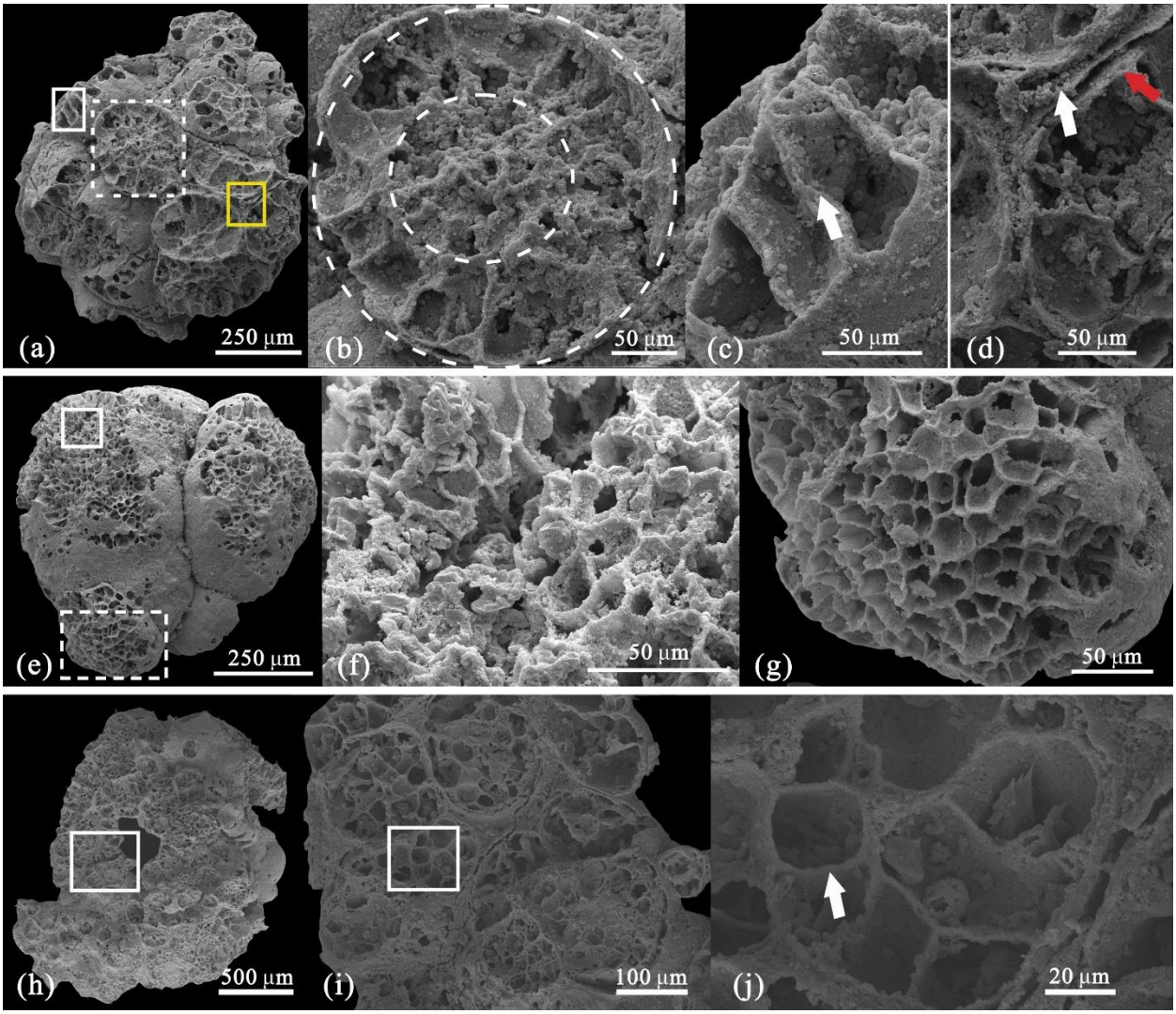

Figure 6. The exposed cell walls of multicellular aggregate fossils from the Cambrian Kuanchuanpu Formation. (a–d), No. ELISN166-86, multicellular aggregate fossils, the image shows the structure of the multicellular clumps; (b), (c), (d) are magnifications of the white solid frame, white dotted frame, and yellow frame in (a), respectively. (b) Cylindrical and square columns of the outer cells that are radially arranged between two concentric circles; the spherical-like inner cells are arranged in a reticular pattern within the small concentric circles; (c) the gap between adjacent cells (white arrow); (d) the organic matter membrane between multicellular

clumps (white arrow), and the cell wall (red arrow). (e–g), No. ELISN166-422, an aggregate fossil with cells arranged in a honeycomb pattern; (f), (g) are close-up view of the white solid frame, white dotted frame in (e), respectively. (h–j), morphology and cell arrangement of amorphous aggregate fossil specimen No. ELISN167-201; (i), (j) are magnifications of the white solid frame in (h) and (i), respectively.

5. Discussion

5.1. Biological affinities

5.1.1 Cyanobacterial hypothesis

Spheriform colonial fossils are widespread in the Proterozoic to Cambrian rocks and are frequently interpreted as bacterial colonies (Butterfield, 2015; Sergeev and Schopf, 2010). For example, many sphaeromorphic colonial fossils (e.g. *Myxococcoides*) from the Kuanchuanpu Formation, including diverse microfossils of heterogeneous origin (e.g. cyanobacteria) and unknown hollow microbial sheaths (Cui et al., 2020), have been difficult to classify taxonomically. The aggregate fossils described herein superficially resemble cyanobacteria based on the external colloid sheath/gelatinous membrane and the aggregate preservation. Therefore, it comes first to determine whether the aggregate fossils described herein represented prokaryotes or eukaryotes by comparing their size, cellular differentiation, and individuality.

Size often takes a central role in discerning fossil eukaryotes and prokaryotes. The cells in modern spheroidal cyanobacteria are approximately 1–55 μm and commonly about 4 μm in diameter (Schopf and Oehler,1976). The cells in cyanobacterial colonies are typically uniform in size, except for a few enlarged heterocysts (Golubic et al., 2000). Cyanobacteria fossils such as *Gloeodiniopsis* in the Kuanchuanpu Formation are approximately 9–20 μm (Cui et al., 2020). In contrast, the cells in the aggregate fossil described herein range from 5 to 50 μm in size, and such a wide variation was unknown in cyanobacterial colonies.

Cell differentiation is one of the most important criteria to distinguish multicellular organisms from the colonial form of unicellular prokaryotes (Zhang, 1989). We can recognize morphologically two distinct types of cells in each multicellular unit of the aggregate fossils. The outer cells are mostly elongate cylindrical in shape, arranged in a radiate palisade along the margin of each multicellular unit; and they are much bigger and dramatically different from the fusiform inner cells. Therefore, the agglomerate fossils examined herein undoubtedly represent a multicellular organism.

5.1.2 Metazoan embryo hypothesis

As discussed above, the aggregate fossils described herein likely represent higher eukaryotes, particularly animal embryos or multicellular algae. In the Kuanchuanpu biota, metazoan embryos fossils from blastocyst to larvae were reported and generally accepted for their synapomorphies (Yue and Bengtson, 1998; Bengtson and Yue, 1997). These agglomerate fossils exhibit

a distinct "cleavage-like" structure, which is superficially similar to metazoan embryo fossils in the early cleavage stage. Although determining the biological identities of aggregate fossils remains a considerable challenge, the aggregate fossils studied herein can still be identified based on their size, shape, cell cleavage, external membrane, and cell wall.

(1) Size: the aggregate fossils studied herein are inconsistent with co-occurred embryo fossils in size. Most animal embryo fossils from the Kuanchuanpu Formation are approximately 590–910 μm in diameter, and only a few embryos range from 1250 to 1690 μm (Steiner et al., 2004b, 2014). The aggregate fossils range from 500 μm to 2900 μm in maximal length and 350–2000 μm in maximal width, much larger than the co-occurred animal embryos.

(2) Shape: the Cambrian animal embryos with a cleavage-like structure were known to possess an egg envelope even in thickness (see Han et al., 2013, 2016b). Therefore, the soft tissue is restricted to a spherical egg envelope. In contrast, although the aggregate fossils are encapsulated by a thin organic membrane (Fig. 2), its amorphous shape and growth in random directions (Fig. 3) are inconsistent with animals or animal embryos with defined configurations.

(3) Cell cleavage: the cell cleavage pattern is among the most important factors to determine the biological affinities of microfossils. Metazoan embryos generally exhibit a pattern of palintomic cell cleavage without cytoplasmic growth. Through successive cell proliferation, a single cell may build a stereoblastula-like structure with hundreds of daughter cells within. These daughter cells are spherical with smooth edges and loosely arranged, making it difficult to trace the sequence of cell divisions as lacking identifiable major division furrows (Stern, 2004). By contrast, the cells of the aggregate fossils are tightly packed with each other and are delimited by polygonal boundaries or furrows (Fig. 6f); moreover, the sequence of multistage cell divisions is quite distinct from that of animals.

(4) External membrane: the entire metazoan embryo during the cell division stages is generally covered by an independent egg envelope with a constant thickness (Fig. 1f) and it is more resistant than soft-tissue of the enclosed embryos. By contrast, the external organic membrane of the agglomerate fossils can extend into the gap between multicellular units (Fig. 5b, g, h), unlike the egg envelope of an animal embryo. It is worthy of noting that the organic membrane is unlikely a diagenetic coating constituted by one or several layers of acicular apatite crystals (see Fig. 4.1 in Steiner et al., 2014) with regard to the exclusive occurrence of the homogenous composition in current aggregate fossils and its absence in other co-occurred small shelly fossils. Therefore, the examined structures most likely represent the organic structure originally secreted by the organisms.

(5) The cell wall is the most fundamental difference between agglomerate fossils and animals. Animal cells are devoid of cell walls and are generally only equipped with a protein cell membrane, 7–8 nm in thickness. In the agglomerate fossils, some outer walls appear as square columns (Fig. 6j), indicating that the outer organic wall had a certain thickness and stiffness

comparable to that of a cell wall. If this is true, the interpretation of the agglomerate fossils as animal embryos appears unlikely.

5.1.3 Multicellular algae hypothesis

Based on the external membranes, cell differentiation, and cell wall structure, the fossil aggregates are most likely multicellular algae.

First, the organic membrane of the agglomerate fossils is very common in eukaryotic algae (Barsanti and Gualtieir, 2006), whose cells are encapsulated by a colloid coating that is very similar to the organic membrane in the aggregate fossils. Second, the cells of the multicellular units differentiate into outer and inner layers in the agglomerates (Fig. 5). In the outer layer, the close-packed pyramidal cells diverge radially from the sphere center to the surface; the vertical cell rows expand outward to form a fountain-like anatomical array (Fig. 5c), which is reminiscent of a "cell fountain", a distinctive hallmark of pseudo-parenchymatous growth in extant red and brown algae (see Bold and Wynne, 1985). The cells in the inner layer are spherical, spheroidal, or spindle-shaped, and are significantly smaller than those in the outer layer and irregularly arranged (Fig. 5g–j). This double-layered structure is similar to the cortex and medulla of multicellular algae (Zhang, 1989). Finally, the inferred cell wall, pyramidal shape, distinct stiffness, and decay resistance of the fossil aggregates favor the interpretation of the aggregate fossils as the multicellular algae. However, a more detailed comparison with modern algae cannot be conducted due to the lack of biochemistry and subcellular fraction evidence. Nonetheless, a comparison between our samples and exceptionally preserved Precambrian algae (e.g. the Weng'an biota in the Doushantuo phosphorites, China) may provide informative clues.

The Weng'an biota is remarkably rich in cellularly preserved multicellular algae including *Wengania globosa*, *Wengania exquisite*, *Thallophyca corrugate* (Zhang, 1989), *Gremiphyca corymbiata* (Zhang et al.,1998), *Thallophycoides phloeatus* (Zhang and Yuan, 1992). Based on the characteristics of well-preserved pseudoparenchyma, apical meristem, parenchyma, and complex thallus with cortex-medulla differentiation, as well as the reproductive tissues (carpospores, carposporangia, and conceptacles), *Wengania*, *Gremiphyca*, *Thallophycoides* and *Thallophyca* in Weng'an biota were classified as Florideophyceae (Rhodophyta) (Zhang et al., 1989; Zhang et al., 1998; Xiao, 2004; Yuan et al., 2002).

There are striking similarities between the above-mentioned Weng'an algae and aggregate fossils in the Kuanchuanpu biota. (1) Thallus shape similarities. Although the shape of the thallus in Weng'an biota is ambiguous based on random thin section (i.e. two-dimensional) observations, the consistently circular outline of thalli observed in the thin sections suggests that *Wengania* tend to be nodular and lumpy or that other more complex thalli may co-exist in the same assemblage (Yuan et al., 2002; Xiao et al., 2004). Moreover, the aggregate fossils in the Kuanchuanpu biota are constituted of sphere-shaped or lump-shaped units. Particularly, the double-sphere shape of *Wengania globosa* obtained in the Doushantuo Formation in Shaanxi Province (Fig. 9 in Xiao et

al., 2004) is congruent with the specimen in Fig. 2c. Additionally, the spatial configuration of multicellular units in *Gremiphyca corymbiata* (Figs. 12–14 in Xiao, 2004), resembles that of the agglomerate fossils of the Kuanchuanpu biota (Figs. 3, 6). (2) Size similarities. *W. globosa* thalli in thin sections range from 70 to 750 μm in diameter (Xiao et al., 2002). In the Kuanchuanpu biota, although the size of the lumps in the agglomerate fossils range from 30 to 500 μm (i.e. slightly smaller than the dimensions associated with *W. globosa*), they are still very close to the sizes expected in *W. globosa*. (3) Cell differentiation. The samples had a similar "cell fountain"-like arrangement and double-layer differentiation, forming the cortex and medulla of the thallus (Figs. 4, 5 in Xiao et al., 2004).

Notably, there are some distinctions between the agglomerate fossils in the Kuanchuanpu biota and the multicellular algae in the Weng'an biota. (1) The organic membrane is absent in Weng'an algae, although a potential of a taphonomical artifact cannot be excluded. (2) The apical meristem and reproductive tissues (carpospores, carposporangia, and conceptacles) are absent in the agglomerate fossils studied herein.

In summary, although the agglomerate fossils in the Kuanchuanpu biota exhibit some differences from those in the Weng'an biota, their external morphology, spatial configuration, size, pseudoparenchyma, 'cell fountains', and cortex-medulla differentiation are all suggestive of a close affinity with the Weng'an algae. Therefore, the discovery of agglomerate fossils in the Kuanchuanpu and Weng'an biota tend to support continuous evolution of multicellular algae from the Ediacaran to the early Cambrian, consistent with the evidence provided by the skeletal fossils in Ediacaran-Cambrian boundary (Cai et al., 2019; Laflamme et al., 2013; Yang et al., 2016; Zhu et al., 2017).

5.2. A hypothesized life cycle of asexual reproduction

Although the full-grown, mature forms remain obscure, the large abundance of the aggregate fossils from the Kuanchuanpu Formation allows us to reconstruct their asexual life cycle based on three lines of evidence. First, the sphere-shaped or lump-shaped unit of the aggregate fossils, which is well delimited from adjacent units, is most likely proliferated from a single cell. Second, the proliferation in random direction of these the aggregate fossils and their units can produce a broad scope of morphological variations. Third, the aggregate fossils most likely belong to the same taxon based on amorphous morphology, continuous range of size (Fig. 4), cell division, and the cell differentiation pattern. These fossils can be grouped into three distinct stages of life cycle based on their increasing size and number of multicellular units (Figs. 7, 8).

In the primary stage, the aggregate membrane-bearing algae are spherical or sub-spherical (Figs. 7a, 8a) with uniform size of external cells, indicating a constant speed of proliferation. In the expansion stage, a portion of cells in the outer layer of a single sphere may develop successively inside a common membrane by successive proliferation, thereby forming a non-spherical cauliflower-like elevated bump structure; and lastly, growing into a prominent spherical multi-

cellular unit interpretable as a gemmule. The random formation of new bumps, probably mediated by allometric growth, leads to an amorphous agglomerate configuration composed of multiple multicellular units or gemmules (Figs. 7b–d, 8b–d). In this stage, the organic membrane is restricted to the external surface of the agglomerate. In the relatively mature stage, the outer membrane extends into space among multicellular units. Subsequently, the unit becomes enveloped by its own organic membrane (Figs. 7e–g, 8e–f) that finally detach from the agglomerate and form an independent individual (Figs. 7a, 8a).

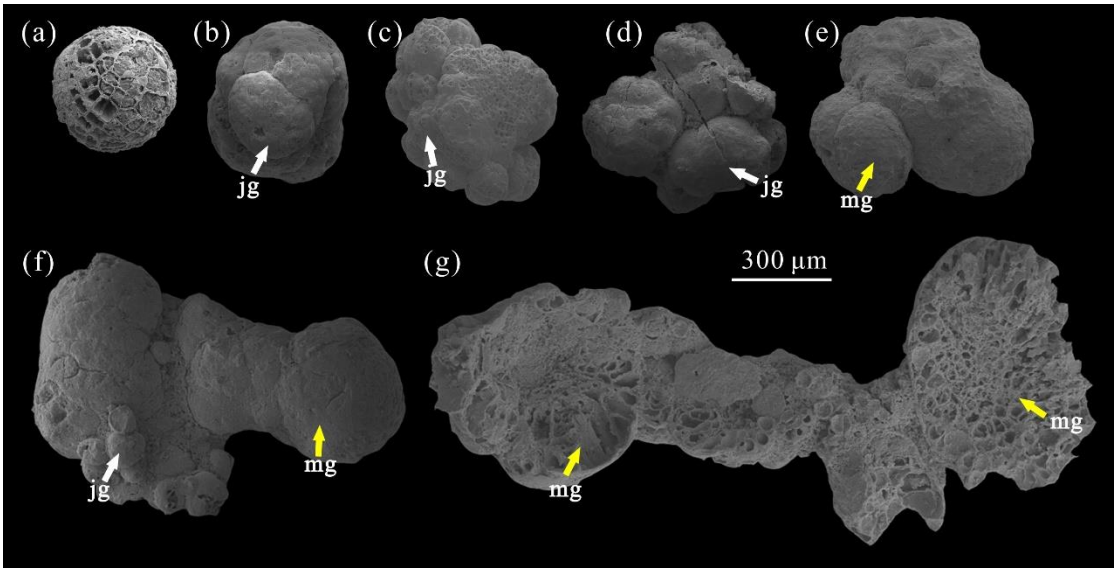

Figure 7. Aggregate fossils in the putative life cycle. (a), an algae fossil in the initial growth stage; (b), an algae fossil in the reproductive stage, with a juvenile gemmule structure (yellow arrow); (c–d), algae fossils in the subsequent allometric growth stage with larger gemmules; (e–g), algae fossils in the relative mature stage exhibiting a mature gemmule (white arrow), which will readily separate from the matrix. All these images share the same scale. jg: juvenile gemmule; mg: mature gemmule.

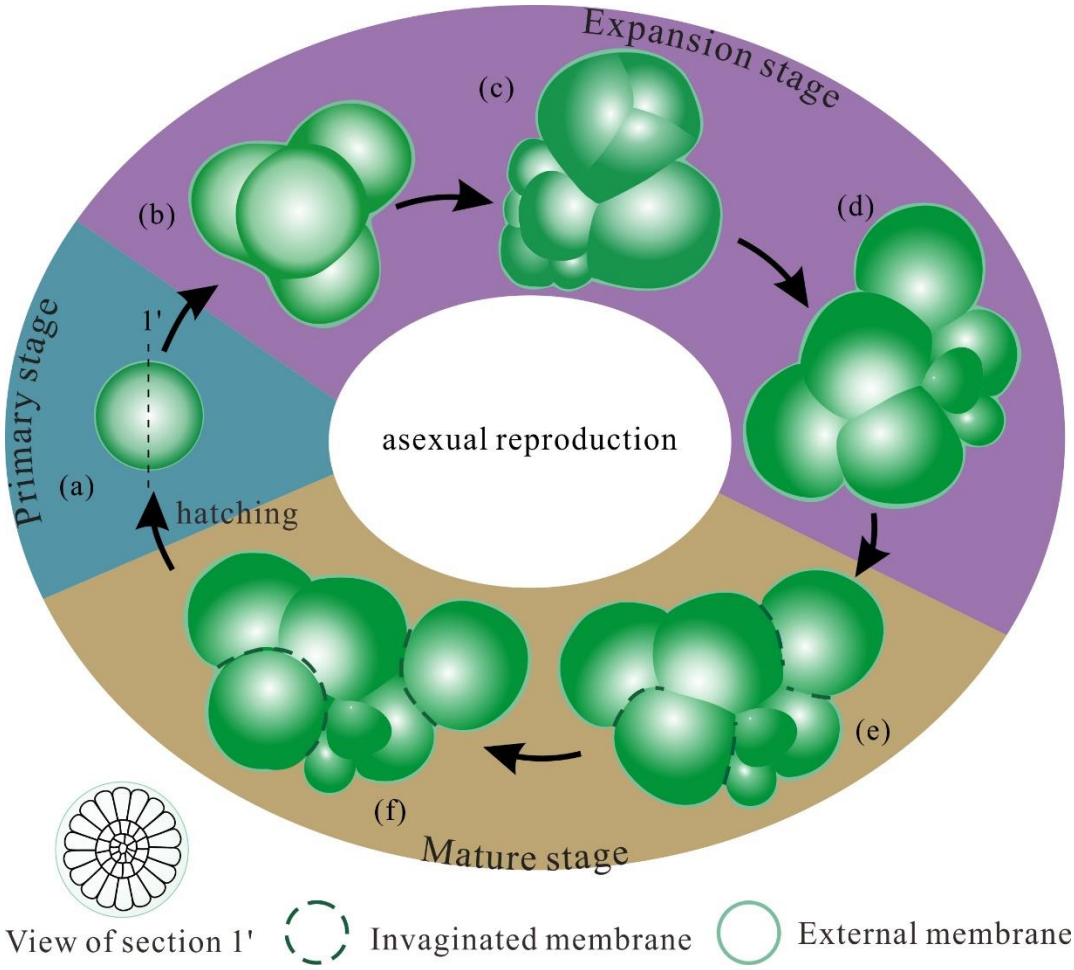

Figure 8. Schematic drawing of the asexual life cycle of the multicellular aggregate algae.

6. Conclusion

Based on the basic morphology, external membranes, spatial configuration, cell differentiation, and particularly the presence of a cell wall, it is more reasonable to interpret the fossil aggregates in the Kuanchuanpu biota as multicellular algae, rather than cyanobacteria or metazoan embryos. The characteristics of the size, morphology, and cortex-medulla differentiation pattern of these agglomerate fossils favor an affinity of Rhodophyta as multicellular algae from the Weng'an biota. We also reconstructed a putative asexual life cycle of these aggregate fossils. The

discovery of agglomerate algae in the Kuanchuanpu biota may provide critical insights for a better understanding of the evolution and fate of the multicellular algae during the Ediacaran–Cambrian transition period. It may provide new evidence on the continuous evolutionary process of Ediacaran and Cambrian creatures.

Acknowledgments

This work was supported by the Strategic Priority Research Program of the Chinese Academy of Sciences (No. XDB26000000), the Natural Science Foundation of China (Nos. 41772010, 41621003, 41672009, 41890844, 41720104002), 111 project of the Ministry of Education of China (No. D17013), and the State Key Laboratory of Palaeobiology and Stratigraphy (Nanjing Institute of Geology and Palaeontology, CAS No.203106). We thank H.J. Gong, J. Luo, and N. Liu (SKLCD) for their assistance in both field and lab work. Data available from the Figshare: https://doi.org/10.6084/m9.figshare.13048349.v1.

References

Barsanti, L., & Gualtieri, P. (2006). *Algae: anatomy, biochemistry, and biotechnology*. NewYork: CRC press.

Bengtson, S., Sallstedt, T., Belivanova, V., & Whitehouse, M. (2017). Three-dimensional preservation of cellular and subcellular structures suggests 1.6 billion-year-old crown-group red algae. *PLoS Biol, 15*(3), e2000735. doi:10.1371/journal.pbio.2000735

Bengtson, S., & Yue, Z. (1992). Predatorial Borings in Late Precambrian Mineralized Exoskeletons. *Science, 257*(5068), 367. doi:10.1126/science.257.5068.367

Bengtson, S., & Yue, Z. (1997). Fossilized Metazoan Embryos from the Earliest Cambrian. *Science, 277*(5332), 1645. doi:10.1126/science.277.5332.1645

Bold, H.C., & Wynne, M.J. (1985). *Introduction to the Algae*. Engelwood Cliffs, NJ: Prentice Hall.

Brocks, J. J., Jarrett, A. J. M., Sirantoine, E., Hallmann, C., Hoshino, Y., & Liyanage, T. (2017). The rise of algae in Cryogenian oceans and the emergence of animals. *Nature, 548*(7669), 578–581. doi:10.1038/nature23457

Butterfield, N. J., & Lomax, B. (2015). Proterozoic photosynthesis - a critical review. *Palaeontology, 58*(6), 953–972. doi:10.1111/pala.12211

Cai, Y., S. Xiao., G. Li., & H. Hua. (2019). Diverse biomineralizing animals in the terminal Ediacaran Period herald the Cambrian explosion. *Geology, 47*(4), 380-384. doi:10.1130/g45949.1.

Cui, L., Liu, W., & Zhang, X. (2020). Phosphatized microbial fossils from the lowest Cambrian of South China and their ecological and environmental implications for the Kuanchuanpu biota. *Precambrian Research, 338*. doi:10.1016/j.precamres.2019.105560

Ding, L. (1986). On the occurrence of *Obruchevella* from the formation in early Cambrian of south Shaanxi and its srtatigraphical significance. *Journal of Xi'an College of Geology, 8*(1), 23–26. doi: 10.19814/j.jese.1986.01.003

Ding, L., Li, Y., & Chen, H. (1992). Miaohe biota. In Ding, L., Zhang, L., Li, Y., & Dong, J (Eds.), *The Study of the Late Sinian-Early Cambrian Biota from the Northern Margin of Yangtze Platform* (pp.21–31). Beijing: Scientific and Technical Documents Publishing House.

Fu, D., Tong, G., Dai, T., Liu, W., Yang, Y., Zhang, Y., et al. (2019). The Qingjiang biota-A Burgess Shale-type fossil Lagerstätte from the early Cambrian of South China. *Science, 363*(6433), 1338-1342. doi:10.1126/science.aau8800

Golubic, S., Seong-Joo, L., & Browne, K.M. (2000). Cyanobacteria: architects of sedimentary structures. In Riding, R.E., & Awramik, S.M(Eds.), *Microbial Sediments*(pp. 57–67). Heidelberg: SpringerVerlag.

Guo, J., Li Y., & Shu, D. (2010). Fossil macroscopic algae from the Yanjiahe formation, Terreneuvian of the Three Gorges area, South China. *Acta Palaeontologica Sinica, 49* (3): 336-342. doi:10.19800/j.cnki.aps.2010.03.00

Han, J., Li, G., Kubota, S., Ou, Q., Toshino, S., Wang, X., et al. (2016a). Internal microanatomy and zoological affinity of the Early Cambrian *Olivooides*. *Acta Geologica Sinica-English Edition, 90*(1), 38-65. doi:10.1111/1755-6724.12641

Han, J., Kubota, S., Li, G. X., Ou, Q., Wang, X., Yao, X. Y., et al. (2016b). Divergent evolution of medusozoan symmetric patterns: Evidence from the microanatomy of Cambrian tetramerous cubozoans from South China. *Gondwana Research, 31*, 150–163. doi:10.1016/j.gr.2015.01.003

Han, J., Kubota, S., Li, G., Yao, X., Yang, X., Shu, D., et al. (2013). Early Cambrian Pentamerous Cubozoan Embryos from South China. *PLoS One, 8*(8), e70741. doi:10.1371/journal.pone.0070741

Han, J., Morris, S. C., Ou, Q., Shu, D., & Huang, H. (2017). Meiofaunal deuterostomes from the basal Cambrian of Shaanxi (China). *Nature, 542*(7640), 228–231. doi:10.1038/nature21072

Hou, X., et al. (2017). *The Cambrian Fossils of Chengjiang, China –The Flowering of Early Animal Life*. Wiley Blackwell.

Kumar, S. (2001). Mesoproterozoic megafossil *Chuaria–Tawuia* association may represent parts of a multicellular plant, Vindhyan Supergroup, Central India. *Precambrian Research, 106*(3), 187-211. doi:10.1016/S0301-9268(00)00093-0

Yasui, K., Reimer, J. D., Liu, Y., Yao, X., Kubo, D., Shu, D., et al. (2013). A Diploblastic Radiate Animal at the Dawn of Cambrian Diversification with a Simple Body Plan: Distinct from Cnidaria? *PLoS, ONE 8*(6): e65890. doi:10.1371/journal.pone.0065890

Laflamme, M., S. A. F. Darroch., S. M. Tweedt., K. J. Peterson., & D. H. Erwin. (2013). The end of the Ediacara biota: Extinction, biotic replacement, or Cheshire Cat?. *Gondwana Research, 23*(2), 558-573. doi:10.1016/j.gr.2012.11.004.

Li, Y., & Ding, L. (1992). Kuanchuanpu biota, In Ding, L., Zhang, L., Li, Y., & Dong, J(Eds.), *The Study of the Late Sinian-Early Cambrian Biota from the Northern Margin of Yangtze Platform*(pp.64–74). Beijing: Scientific and Technical Documents Publishing House.

Liu, Y., Li, Y., Shao, T., Hu, H., Bai, J., Zhang, W., et al. (2014). The new record of phosphatized *Cambricodium* fossils from the basal Cambrian of the southern Shaanxi, China. *Acta Micropalaeontologica Sinica, 31*(1), 98–103.

Qian Y. (1999). *Taxonomy and biostratigraphy of Small Shell Fossils in China*. Beijing: Science Press.

Qian, Y., Li, G., Jiang, Z., Chen, M., & Yang, A. (2007). Some phosphatized cyanobacterian fossils from the basal Cambrian of China. *Acta Micropalaeontologica Sinica, 24*(2), 222–228.

Sanchez-Baracaldo, P., Raven, J. A., Pisani, D., & Knoll, A. H. (2017). Early photosynthetic eukaryotes inhabited low-salinity habitats. *Proc Natl Acad Sci U S A, 114*(37), E7737–E7745. doi:10.1073/pnas.1620089114

Schopf, J. W., & Oehler, D. Z. (1976). How Old Are the Eukaryotes? *Science, 193*(4247), 47. doi:10.1126/science.193.4247.47

Sergeev, V. N., & Schopf, J. W. (2017). Taxonomy, paleoecology and biostratigraphy of the late Neoproterozoic Chichkan microbiota of South Kazakhstan: the marine biosphere on the eve of metazoan radiation. *Journal of Paleontology, 84*(3), 363–401. doi:10.1666/09-133.1

Shang, X., Liu, P., Moczydłowska, M., Yang, B., & Butterfield, N. J. (2020). Algal affinity and possible life cycle of the early Cambrian acritarch *Yurtusia uniformis* from South China. *Palaeontology*. doi:10.1111/pala.12491

Sharma, M., Mishra, S., Dutta, S., Banerjee, S., & Shukla, Y. (2009). On the affinity of Chuaria–Tawuia complex: A multidisciplinary study. *Precambrian Research, 173*(1–4), 123-136. doi:10.1016/j.precamres.2009.04.003

Sharma, M., & Shukla, Y. (2009). Taxonomy and affinity of Early Mesoproterozoic megascopic helically coiled and related fossils from the Rohtas Formation, the Vindhyan Supergroup, India. *Precambrian Research, 173*(1–4), 105-122. doi:10.1016/j.precamres.2009.05.002

Shen, L., Yin, J., & Zhang, T. (1987). Phosphatic fossil algae from phosphorite deposit in eastern Yunnan. *Journal of Chengdu College of Geology, 14*(3), 11–22.

Steiner, M., Li, G., Qian, Y., & Zhu, M. (2004). Lower Cambrian Small Shelly Fossils of northern Sichuan and southern Shaanxi (China), and their biostratigraphic importance. *Geobios, 37*(2), 259–275. doi:DOI 10.1016/j.geobios.2003.08.001

Steiner, M., Qian, Y., Li, G., Hagadorn, J. W., & Zhu, M. (2014). The developmental cycles of early Cambrian Olivooidae fam. nov (?Cycloneuralia) from the Yangtze Platform (China). *Palaeogeography Palaeoclimatology Palaeoecology, 398*, 97–124. doi:10.1016/j.palaeo.2013.08.016

Steiner, M., Zhu, M., Li, G., Qian, Y., & Erdtmann, B. D. (2004). New early Cambrian bilaterian embryos and larvae from China. *Geology, 32*(10), 833-836. doi:Doi 10.1130/G20567.1

Stern, C. D. (2004). *Gastrulation from cells to embryo*. New York: Cold Spring Harbor Laboratory Press.

Tang, F., Yin, C., & Gao, Z. (1997). A new ideal of Sinian Doushantuo'an metaphyte fossils from Xiuning, Anhui Province. *Acta Geologica Sinica, 71*(4), 491–501.

Tang, F., Yin, C., Liu, P., Wang, Z., & Gao, L. (2007). Discovery of diverse macrofossil assemblages from the Jiucheng Member of uppermost Ediacaran in eastern Yunnan. *Journal of Palaeogeography(Chinese Edition), 9*(5), 533–540.

Tang, Q., Pang, K., Yuan, X., & Xiao, S. (2020). A one-billion-year-old multicellular chlorophyte. *Nat Ecol Evol, 4*(4), 543-549. doi:10.1038/s41559-020-1122-9

Walter, M. R., Oehler, J.H., & Oehler, D.Z. (1976). Megascopic algae 1300 million years old from the Belt Supergroup, Montana: A reinterpretation of Walcott's Helminthoidichnites. *Journal of Paleontology, 50*, 872–881.

Wang, Y., Wang, X., & Huang, Y. (2007). Macroscopic algae from the Ediacaran Doushantuo Formation in northeast Guizhou, South China. *Earth Science Journal of China University of Geosciences, 32*(6), 829–844.

Xiao, S., & Knoll, A. H. (1999). Fossil preservation in the Neoproterozoic Doushantuo phosphorite Lagerstatte, South China. *Lethaia, 32*(3), 219–240. doi:10.1111/j.1502-3931.1999.tb00541.x

Xiao, S., Knoll, A. H., Yuan, X., & Pueschel, C. M. (2004). Phosphatized multicellular algae in the Neoproterozoic Doushantuo Formation, China, and the early evolution of florideophyte red algae. *Am J Bot, 91*(2), 214–227. doi:10.3732/ajb.91.2.214

Xiao, S., Yuan, X., Steiner, M., & Knoll, A. H. (2002). Macroscopic Carbonaceous Compressions in a Terminal Proterozoic Shale: A Systematic Reassessment of the Miaohe Biota, South China. *Journal of Paleontology, 76*(2), 347–376. doi:10.1666/0022-3360(2002)076<0347:Mcciat>2.0.Co;2

Yang, B., M. Steiner., M. Zhu., G. Li., J. Liu., & P. Liu. (2016). Transitional Ediacaran–Cambrian small skeletal fossil assemblages from South China and Kazakhstan: Implications for chronostratigraphy and metazoan evolution. *Precambrian Research, 285*, 202-215. doi:10.1016/j.precamres.2016.09.016.

Yang, X., & Han, J. (2017). Ambient inclusion trails and microboring structures on Early Cambrian microfossils. *Chinese Science Bulletin, 62*(35), 4179–4188. doi:10.1360/n972017-00696

Yang, R., Zhao, Y., Guo, Q., & Shi, G. (1999). Early-Middle Cambrian macroalgal fossils from Taijiang county, Guizhou, China. *Geological Review, 45*(3), 282–290. doi:10.16509/j.georeview.1999.03.010

Yang, R., Mao, J., Zhao, Y., Chen, X., & Yang, X. (2001). Branching macroalgal fossils of the early-middle Cambrian Kaili formation from Taijiang, Guizhou province, China. *Acta Geologica Sinica, 75*(4), 433–440.

Yin, L. (1987). New date of microfossils from Precambrian-Cambrian cherts in Ningqiang, southern Shaanxi. *Acta Palaeontologica Sinica, 26*(2), 87–195. doi:10.19800/j.cnki.aps.1987.02.009

Yuan, X., Xiao, S., Li, J., Yin, L., & Cao, R. (2001). Pyritized chuarids with excystment structures from the late Neoproterozoic Lantian formation in Anhui, South China. *Precambrian Research, 107*(3), 253–263. doi:10.1016/S0301-9268(00)00144-3

Yuan, X., et al. (2002). *Doushantuo Fossils: Life on the Eve of Animal Radiation*. Hefei: China University of Science and Technology Press.

Yuan, X., et al. (2016). *The Lantian Biota*. Shanghai: Shanghai Scientific and Technical Publishers.

Yue, Z., & Bengtson S. (1998). Phosphatized metazoan embryo fossils in Cambrian Explosion. *Chinese Science Bulletin, 43*(17),1858–1882.

Zhao, Y., Chen, M., Peng, J., Yu, M., He, M., Wang, Y., et al. (2004). Discovery of a Miaohe-type Biota from the Neoproterozoic Doushantuo formation in Jiangkou County, Guizhou Province, China. *Chinese Science Bulletin, 49*(18), 2224–2226. doi:10.1007/BF03185792

Zhang, H., & Dong, X. (2015). The oldest know larva and its implications for the plesiomorphy of metazoan development. *Science Bulletin, 60*(22), 1947–1953. doi:10.1007/s11434-015-0886-9

Zhang, Y. (1989). Multicellular thallophytes with differentiated tissues from Late Proterozoic phosphate rocks of South China. *Lethaia*, *22*(2), 113–132. doi:10.1111/j.1502-3931.1989.tb01674.x

Zhang, Y., & Yuan. X. (1992). New data on multicellular thallophytes and fragments of cellular tissues from Late Proterozoic phosphate rocks, South China. *Lethaia, 25*(1), 1-18. doi:10.1111/j.1502-3931.1992.tb01788.x

Zhang, Y., Yin, L. M., Xiao, S. H., & Knoll, A. H. (1998). Permineralized fossils from the terminal Proterozoic Doushantuo Formation, south China. *Journal of Paleontology*, *72*(4), 1–52.

Zheng, Y., Yao, X., Han, J., & Guo, J. (2017). Microscopic fossils with multi-level tetrad cell structures from the Cambrian Kuanchuanpu Formation in South Shaanxi. *Acta Palaeontologica Sinica, 56*(4), 440–448. doi:10.19800/j.cnki.aps.2017.04.005

Zhu, M., A. Y. Zhuravlev., R. A. Wood., F. Zhao., & S. S. Sukhov. (2017). A deep root for the Cambrian explosion: Implications of new bio- and chemostratigraphy from the Siberian Platform. *Geology, 45*(5), 459-462. doi:10.1130/g38865.1.

Zhu, S., Zhu, M., Knoll, A. H., Yin, Z., Zhao, F., Sun, S., et al. (2016). Decimetre-scale multicellular eukaryotes from the 1.56-billion-year-old Gaoyuzhuang Formation in North China. *Nat Commun, 7*(1), 11500. doi:10.1038/ncomms11500